NASA TECHNICAL NOTE

EFFECTS OF THREE TRANSMISSION MODELS IN THE ROTATIONAL WATER-VAPOR BAND ON RADIANCE CALCULATIONS AND CONSTITUENT INFERENCES

by Ruth I. Whitman

Langley Research Center
Hampton, Va. 23365

NATIONAL AERONAUTICS AND SPACE ADMINISTRATION • WASHINGTON, D. C. • APRIL 1971

0133237

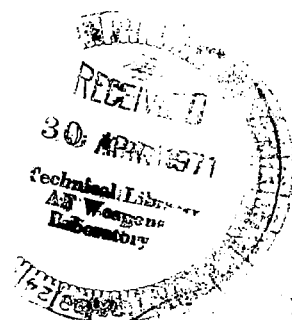| 1. Report No. NASA TN D-6112	2. Government Accession No.	3. Recipient's Catalog No.
4. Title and Subtitle EFFECTS OF THREE TRANSMISSION MODELS IN THE ROTATIONAL WATER-VAPOR BAND ON RADIANCE CALCULATIONS AND CONSTITUENT INFERENCES		5. Report Date April 1971
		6. Performing Organization Code
7. Author(s) Ruth I. Whitman		8. Performing Organization Report No. L-7374
9. Performing Organization Name and Address NASA Langley Research Center Hampton, Va. 23365		10. Work Unit No. 715-02-00-01
		11. Contract or Grant No.
12. Sponsoring Agency Name and Address National Aeronautics and Space Administration Washington, D.C. 20546		13. Type of Report and Period Covered Technical Note
		14. Sponsoring Agency Code

15. Supplementary Notes

16. Abstract

The effects of the Elsasser transmission model, the Bolle-Smith transmission model, and the Goody transmission model on the water-vapor mixing ratios inferred from horizon radiance profiles measured during the NASA Project Scanner flight (August 1966) over a latitude range from 17° N to 58° N are presented. The effects of these transmission models on the calculation of radiance and the inference of water-vapor mixing ratios in the 315 cm^{-1} to 475 cm^{-1} rotational water vapor band and in the 200 cm^{-1} to 300 cm^{-1} rotational water vapor band are shown. A significant mixing ratio profile shape variation exists when the Bolle-Smith transmission model is used instead of the Elsasser transmission model. This mixing ratio profile variation exists because of the difference in the shape of the two transmission models when the transmission is high; thus, the altitude at which this condition occurs is a function of frequency. It does not appear that the shape of the mixing ratio profile would change significantly as a function of band choice if the Goody transmission model were used. Coefficients for a temperature correction for the Goody transmission model are presented.

By using the Goody model, the mixing ratio for the 315 cm^{-1} to 475 cm^{-1} band is essentially independent of altitude above the tropopause over the range of latitudes measured. All three models indicate that below the tropopause, latitude plays a significant role, the highest mixing ratios of these summer measurements occurring at the lower latitudes.

17. Key Words (Suggested by Author(s)) Inference Atmospheric constituents Stratosphere Water vapor Transmission models	18. Distribution Statement Unclassified — Unlimited

19. Security Classif. (of this report) Unclassified	20. Security Classif. (of this page) Unclassified	21. No. of Pages 26	22. Price* $3.00

EFFECTS OF THREE TRANSMISSION MODELS IN THE
ROTATIONAL WATER-VAPOR BAND ON RADIANCE
CALCULATIONS AND CONSTITUENT INFERENCES

By Ruth I. Whitman
Langley Research Center

SUMMARY

The effects of the Elsasser transmission model, the Bolle-Smith transmission model, and the Goody transmission model on the water-vapor mixing ratios inferred from horizon radiance profiles measured during the NASA Project Scanner flight (August 1966) over a latitude range from 17° N to 58° N are presented. The effects of these transmission models on the calculation of radiance and the inference of water-vapor mixing ratios in the 315 cm^{-1} to 475 cm^{-1} rotational water-vapor band and in the 200 cm^{-1} to 300 cm^{-1} rotational water-vapor band are shown. A significant mixing ratio profile shape variation exists when the Bolle-Smith transmission model is used instead of the Elsasser transmission model. This mixing ratio profile variation exists because of the difference in the shape of the two transmission models when the transmission is high; thus, the altitude at which this condition occurs is a function of frequency. It does not appear that the shape of the mixing ratio profile would change significantly as a function of band choice if the Goody transmission model were used. Coefficients for a temperature correction for the Goody transmission model are presented.

By using the Goody model, the mixing ratio for the 315 cm^{-1} to 475 cm^{-1} band is essentially independent of altitude above the tropopause over the range of latitudes measured. All three models indicate that below the tropopause, latitude plays a significant role, the highest mixing ratios of these summer measurements occurring at the lower latitudes.

INTRODUCTION

The objective of the NASA Project Scanner was to measure horizon radiance profiles of the earth which would provide a better understanding of the primary input to horizon-sensing devices. Horizon radiance profiles were measured in two spectral bands of the strongly absorbing atmospheric constituents: 615 cm^{-1} to 715 cm^{-1} of the carbon dioxide (CO_2) molecule and 315 cm^{-1} to 475 cm^{-1} of the water vapor (H_2O) molecule. A

description of the project and the results for the summer measurements obtained from the flight from Wallops Island, Virginia, on August 16, 1966, are given in reference 1. Results for the winter measurement, made from Wallops Island, Virginia, on December 10, 1966, are given in reference 2. An attempt was made to estimate the temperature and pressure structure of the atmosphere in the geographic regions where measurements were taken so that radiance profiles could be independently predicted. Unfortunately, the water-vapor mixing ratio is not routinely measured to altitudes that are sufficiently high to be useful in calculating horizon radiance profiles.

A natural outgrowth of the effort to predict radiance profiles analytically was to reverse the problem and use measured horizon radiance profiles to infer water-vapor mixing ratio in the atmosphere. Any inversion technique that utilizes measured radiance as an input and leads to either atmospheric temperature or an atmospheric constituent amount as an output makes the basic assumption that radiance can be calculated analytically. The basic assumptions made when radiance is computed is that the source function is mathematically describable and that the transmission, absorption, and scattering of the medium between the source and the observer can be calculated.

To facilitate the computation of radiance in the infrared region of the spectrum, local thermodynamic equilibrium has been assumed. This assumption is valid as long as collision effects control the excitation and de-excitation of the atoms and molecules. The assumption affects the radiance calculation in that the source function is Planckian and scattering in the medium can be ignored. Since the source function is specified and the scattering ignored, the major problem left in computing radiance is calculation of the transmission or absorption in the intervening medium. The intervening medium that is of interest is the atmosphere. The calculation of transmittance/absorption is complicated since the atmosphere is complicated. Absorption is temperature and pressure dependent and in a real atmosphere temperature and pressure are variables. The spectrum of each atmospheric constituent that is optically active in the infrared region of the spectrum is made up of many lines whose shapes are functions of temperature and pressure. For these reasons transmission modeling in the infrared region has long been practiced. The accuracy of the radiance calculation is, therefore, a function of the transmission model assumed, and the assumed transmission model is, of necessity, one of the limits on the accuracy of an inversion technique.

A comparison of the relative merits of the basic assumptions implicit in developing a model or the relative merits of a model approach or a system of line by line integration is beyond the scope of this paper. Reference 3 is an excellent discussion of the last point.

In reference 4 it was stated that the absolute value of the inferred water-vapor mixing ratios was dependent upon the transmission model assumed. It further stated that the transmission model that was assumed was chosen because it was available in program form and that an evaluation of errors associated with the choice of the transmittance model was beyond the scope of that paper.

Since the publication of reference 4, two further transmission models have been programed. The effect of various transmission models in the calculation of radiance in the rotational water-vapor band and the effect of the transmittance model on the inversion technique in reference 4 are the subject of this paper.

A short discussion of the effect of the Elsasser transmission model and the Bolle-Smith transmission model on inference work in the 315 cm^{-1} to 475 cm^{-1} region of spectrum is presented in reference 5.

SYMBOLS

a   constant in temperature correction, frequency dependent (as used in ref. 9), $\deg^{-1}$

b   constant in temperature correction, frequency dependent, $\deg^{-2}$

$\left.\begin{array}{l} a_\nu, b_\nu, \\ c_\nu, d_\nu \end{array}\right\}$ constants in polynomial representation of transmission, frequency dependent (as used in ref. 10), dimensionless

i   integer

L_ν generalized absorption coefficient, cm^{-1}

p   pressure, millibars

S   line intensity, cm/g

T   temperature, $^\circ\text{K}$

u   optical depth, cm

u^* reduced optical depth (as used in ref. 6), cm

α_L Lorentz width of spectral line, cm^{-1}

$\phi(T)$ constant in temperature correction of optical depth, dimensionless

τ transmission, dimensionless

τ_ν transmission as a function of bandwidth

ν wave number of band center, cm^{-1}

Subscript:

o   base

Bars over symbols denote average values.

TRANSMISSION MODELS

Three transmission models were chosen for this study. They are presented in chronological order. The first model — the Elsasser model — assumed Lorentz line shape, equal spacing, and equal intensity for the lines. The resulting absorption model varies smoothly not only with gas concentration but also with wave number. The second model — the Goody model — is a random model with a bandwidth of 20 cm^{-1}. It takes variation of line strength and position into consideration. The third model — the Bolle-Smith model — is a polynomial fitted to transmission data. The resolution in this model is 5 cm^{-1}.

Elsasser Model

The Elsasser transmission model (ref. 6) was the transmission model utilized in reference 1. In the Elsasser transmission model the transmission τ is a function of two variables: $L\nu$, the generalized absorption coefficient incorporating the frequency dependency of τ; and u^*, the reduced optical thickness incorporating the pressure dependency of τ

$$\tau_\nu = \tau(L_\nu u^*) \tag{1}$$

The generalized absorption coefficient for the rotational water-vapor band is presented in both graphical and tabular form in reference 6. In reference 4 the bandwidth increments used in radiance calculations were 10 cm^{-1} instead of the 40 cm^{-1} increments

presented in reference 6. The smooth variation of the generalized absorption coefficient in the region of interest enables one to plot the generalized absorption coefficient to obtain the desired resolution. The increments are those used in reference 4. Reference 6 showed that the generalized absorption coefficient was temperature dependent; thus, the temperature correction technique for the generalized absorption coefficient given in reference 7 was used.

Goody Model

The Goody transmission model (ref. 8), which assumes the probability that a line has an intensity between S and $S + \Delta S$ can be expressed as an exponential, has been programed. This Goody transmission model can be expressed as follows:

$$\tau_\nu = \exp \left\{ \frac{-\dfrac{u}{\Delta \nu} \displaystyle\sum_i S(i)}{\dfrac{1}{4} \left(\dfrac{u \displaystyle\sum_i S(i)}{\dfrac{p}{p_0} \displaystyle\sum_i S(i) \, \alpha_L(i)} \right)^{1/2}} \right\} \tag{2}$$

In equation (2) τ_ν is transmission, u is optical depth, $\Delta \nu$ is waveband, p/p_0 is a pressure ratio referred to base pressure, $S(i)$ is the line strength of the ith line in the interval and $\alpha_L(i)$ is the Lorentz width of the ith line in the interval for the base pressure p_0. (Whenever possible, the symbols used by the original author were retained in the interest of clarity.) Temperature varies in the atmosphere; therefore, choice of only one set of $\displaystyle\sum_i S(i)$ and $\displaystyle\sum_i S(i) \, \alpha_L(i)$ for calculation purposes was undesirable. It can be seen that the water-vapor optical depth term u and the summation terms are multiplicative; thus, a temperature correction of the optical depth u instead of the summation terms can effectively correct the τ_ν term for temperature. If an apparent optical depth of the form

$$u_{apparent} = u \phi(T) \tag{3}$$

where $\phi(T)$ is the temperature correction term could be determined and used in equation (2), the transmission could be corrected for temperature. A simple, linear form for $\phi(T)$ did not result in a sufficiently accurate correction; therefore, a temperature correction similar to the one in reference 9 was used:

$$\log_e \phi(T) = \overline{a}(u)(T - 260) + \overline{b}(u)(T - 260)^2 \approx \overline{a}(T - 260) + \overline{b}(T - 260)^2 \qquad (4)$$

where a and b are coefficients, u is optical depth, and T is temperature in ^{O}K.

In reference 8, values of $\sum_i S(i)$ and $\sum_i S(i)\,\alpha_L(i)$ are available for the three temperatures; 220° K, 260° K, and 300° K. For a constant u and a given p/p_0, three values of τ_ν can therefore be calculated from equation (2). At a given p/p_0 the interaction of equations (2) and (4) results in two equations and two unknowns for each value of optical depth. For each wave band, pairs of equations were solved to find a(u) and b(u) for 50 values of optical depth from u = 0.00001 cm to u = 1.0 cm. These values were chosen to allow τ_ν to vary between approximately 0.99 and 0. The values of a and b do not vary greatly as a function of u; therefore, an average $\overline{a}$ and $\overline{b}$ were found for each wave-band interval and are presented in table I. As an example, for the band $\nu = 300$ cm^{-1} to $\nu = 320$ cm^{-1}, a(u) varied between 8.9578×10^{-3} and 8.5968×10^{-3}, b(u) varied between -4.8361×10^{-5} and 4.1172×10^{-5}. Since the constituent inference technique of reference 4 is applicable only where the atmosphere is not opaque, it is desirable that the temperature correction be most accurate in the stratospheric region. To assure that the temperature correction be most accurate for stratospheric cases, more of the 50 optical depths were representative of the short optical depths found in the stratosphere rather than of the longer optical depths representative of the troposphere. The value of τ_ν corrected for temperature in this manner was spot checked in various wave-length regions and was found to differ from the directly calculated transmission in the third or fourth decimal place. In the region of shorter optical depth (higher transmission), the deviation was less than 0.5 percent.

Bolle-Smith Model

The polynomial representation of the Bolle-Smith transmission model presented in reference 10 is the final model used in this comparison. It was shown in reference 10 that the transmission could adequately be written as

$$\tau_\nu = \exp\!\left(-a_\nu\, u^{b_\nu}\, p^{c_\nu}\, T^{d_\nu}\right) \qquad (5)$$

where a_ν, b_ν, c_ν, and d_ν are constants used in reference 10 that are dependent on the frequency ν. A polynomial expression may be obtained by taking the logarithm of equation (5) twice. The coefficients of the resultant polynomial representation of Bolle-Smith transmission model are detailed in reference 10.

Effects of Transmission Models

Transmission model calculations.- Figure 1 presents graphical representations of comparisons between the Goody transmission model, the Bolle-Smith transmission model, and the Elsasser transmission model as a function of wave number when pressure, temperature, and optical depth are constants at sea level and 20 km, respectively. Transmission models are an attempt to obtain a representation of the average transmission over a specific bandwidth instead of attempting to represent the effect of individual line position and strength. It is erroneous to attempt to compare the values of transmission in less than the widest bandwidth shown. For example, the area under the 20 cm^{-1} bandwidth for the Goody model should be compared with the area under the four applicable 5 cm^{-1} intervals of the Bolle-Smith model. As the bandwidth increases, the similarity tends to increase.

Radiance calculations.- The calculation of transmissions in the presence of constant temperature, pressure, and optical depth does not show or explain the effects of applying different transmission models in the calculation of radiance where temperature, pressure, and mixing ratios are varying. A way to determine the effect of applying several transmission models to the calculation of radiance from the earth's limb is to incorporate different transmission models in the same computer program. Figure 2(a) shows the horizon radiance profile in 315 cm^{-1} to 475 cm^{-1} interval and figure 2(b) is the horizon radiance profiles in the 200 cm^{-1} to 300 cm^{-1} interval. Values of temperature and pressure (table II) from the U.S. Standard Atmosphere (ref. 11) were the atmospheric input. Table III shows the mixing ratio that was assumed in reference 4, and the calculated radiances. The basic technique used in calculating the radiances is the same and this technique is explained in reference 7. The band resolution considered for each model is different and corresponds to the resolution depicted in figure 1. In figure 2(a) for 315 cm^{-1} to 475 cm^{-1}, the radiance calculated by using the Goody transmission model is generally greater above the tropopause (approximately 15 km) than the radiance calculated with the other 2 models. From a measured radiance profile, the mixing ratio that is inferred would therefore be less with the use of the Goody transmission model than with the use of the other models. The calculated radiance in this band obtained by using the Bolle-Smith transmission model is less than the calculated radiance obtained by using the Elsasser model between approximately 11 km and 25 km and is greater above 25 km. This result would mean that the inferred mixing ratio using the 315 cm^{-1} to 475 cm^{-1} band above 25 km would be less and that below 25 km would be greater if the Bolle-Smith transmission model was used instead of the Elsasser transmission model. For similar arguments, figure 2(b) $\left(200 \text{ cm}^{-1} \text{ to } 300 \text{ cm}^{-1}\right)$ shows a different relationship. The radiance calculated by use of the Bolle-Smith model does not become greater than the radiance calculated by use of the Elsasser model in the 200 cm^{-1} to 300 cm^{-1} band until approximately 40 km.
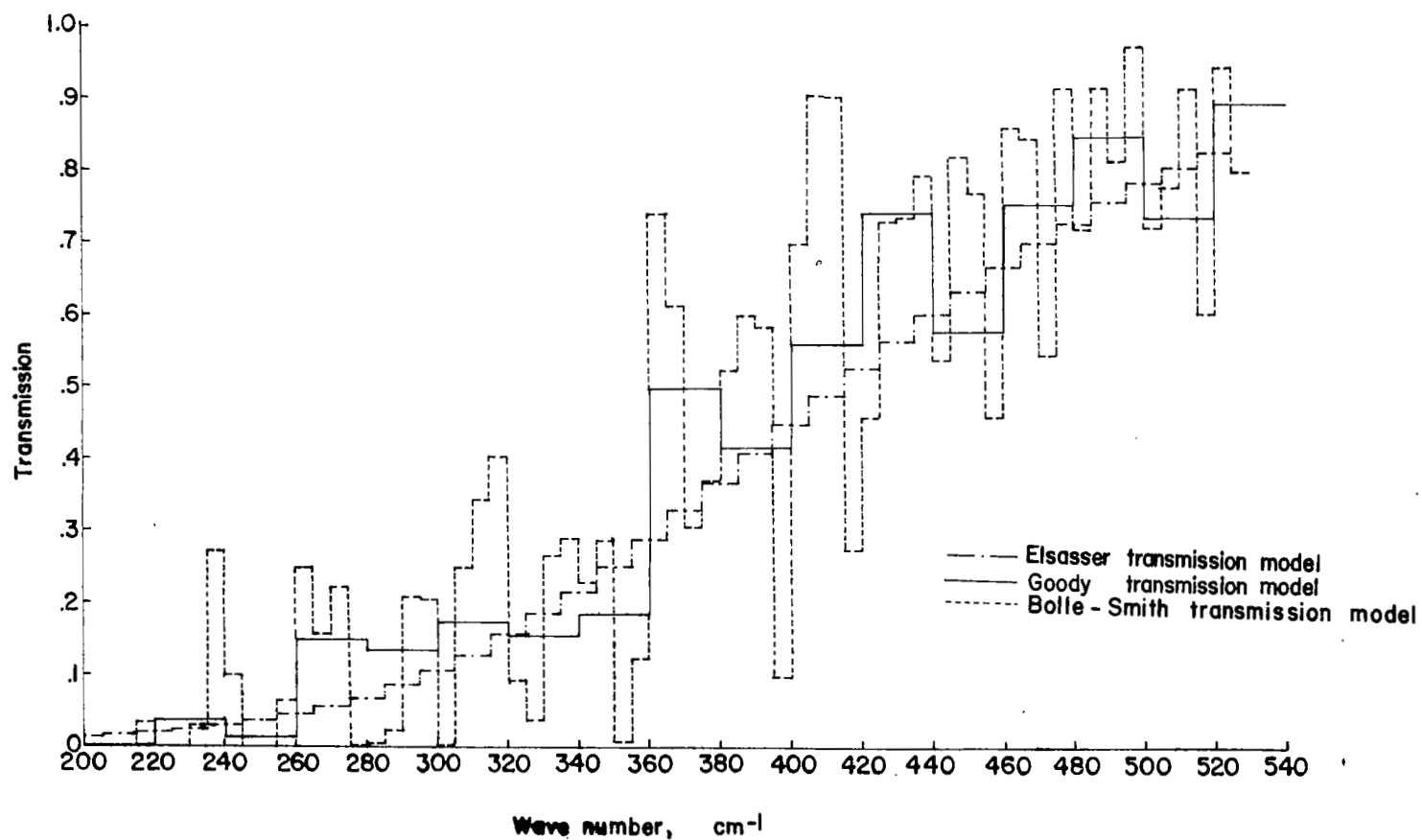
(a) Sea level (p = 1000 mb, T = 260° K, u = 0.02 cm).

Figure 1.- Comparison of transmission models at constant temperature, pressure, and optical depth.
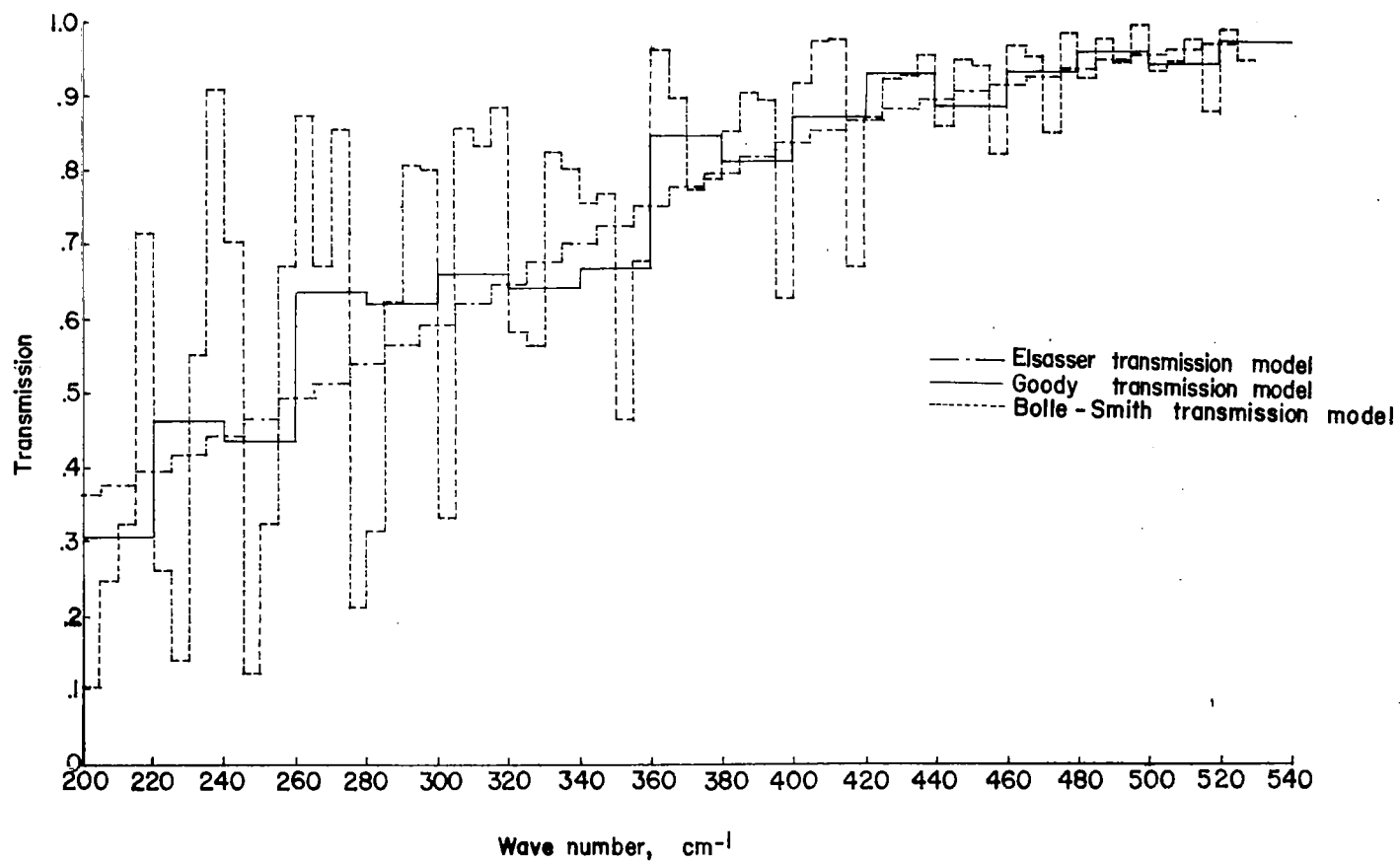
(b)   20 km (p = 55.29 mb,   T = 260° K,   u = 0.02 cm).

Figure 1.- Concluded.

The average transmission for the band at the crossover point in figure 2(a) is greater than 0.9, thus, the mixing ratio inferred above 25 km in the 315 cm^{-1} to 475 cm^{-1} region is a function of the shape of the transmission curve between $\tau_\nu = 0.9$ and $\tau_\nu = 1.0$ in the assumed transmission model. Transmission data are less accurate where
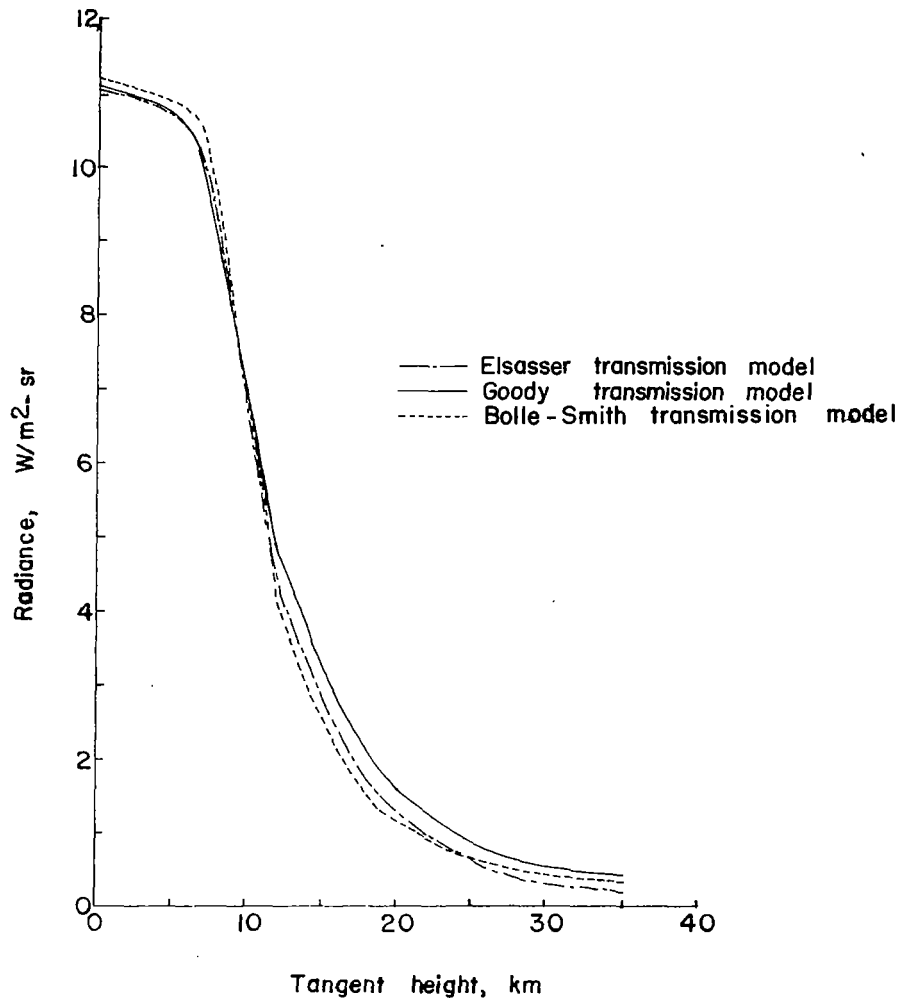
(a)   315 cm^{-1} to 475 cm^{-1}.

Figure 2.- Radiance profiles calculated by using 1962 U.S. Standard Atmosphere, a standard mixing ratio, and different transmission models.

large changes in optical depth result in small changes in transmission. This condition occurred between $\tau_\nu = 0.9$ and $\tau_\nu = 1.0$. A comparison of figures 2(a) and 2(b) shows that the inferred mixing ratio in the 25 km to 45 km range would strongly depend on the transmission model chosen. The bandwidth of the measurements should be chosen to optimize the range of τ_ν variation for inversion purposes.

Further theoretical and experimental determination of line strength and position plus experimental determination of the transmission in the rotational water-vapor band under conditions of short optical depth and low pressure are required before final determination of the best transmission model is made.
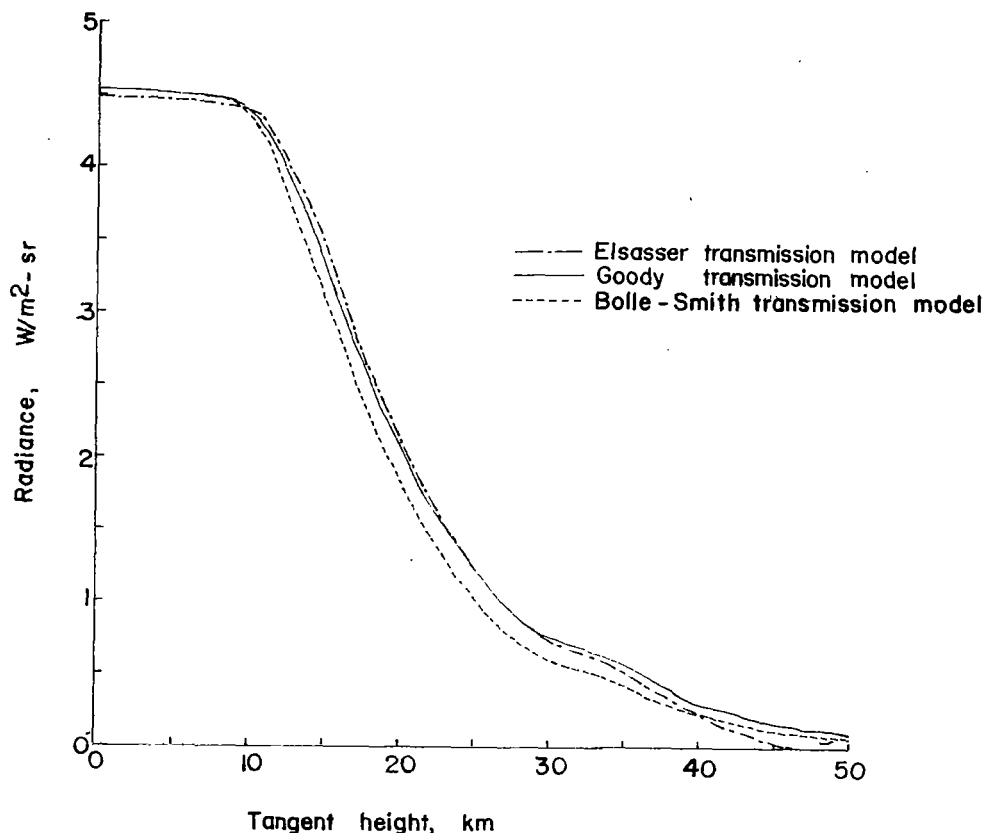
(b)   200 cm^{-1} to 300 cm^{-1}.

Figure 2.- Concluded.

Mixing Ratios From Project Scanner

To illustrate the effect of different transmission models on the inferred mixing ratios, mixing ratios were inferred from the radiance profiles measured for the 315 cm^{-1} to 475 cm^{-1} spectral interval in NASA Project Scanner. Only the transmission model was varied. The accuracy of the radiance data in the 315 cm^{-1} to 475 cm^{-1} region and a discussion of the associated meteorological data from Project Scanner have been discussed in reference 1.

The horizon radiance profiles were measured on a rocket probe launched from the NASA Wallops Station at 0618 GMT on August 16, 1966. Measured horizon radiance profiles were grouped into seven geographic cells which were centered at the following locations:

	Values for geographic cell —						
	1	2	3	4	5	6	7
Latitude, ^{O}N	58	53	47	43	35	21	17
Longitude, ^{O}W	68	60	57	45	48	55	60

The radiance profiles are reproduced from reference 1 in table IV and the associated meteorological data is reproduced in table V. Table VI gives the inferred mixing ratios when the Goody and the Bolle-Smith transmission models were used and also reproduces the mixing ratios inferred using the Elsasser transmission model previously reported in reference 4. Figure 3 is a graphical presentation of cell 5, used as an example, of the effect of using different transmission models. Some of the more recently reported measurements of mixing ratios in the stratosphere (refs. 12, 13, 14, and 15) are also shown in figure 3. The mixing ratios inferred with the technique of reference 1 using the Elsasser transmission model, the Goody transmission model, and the Bolle-Smith transmission model are within factors of 2 to 3 of each other and within factors of 2 to 5 of other measurements but are consistently above the other measurements. The inferred mixing ratios indicate that the stratosphere is dryer than the stratospheric mixing ratio proposed as the Chico mean (ref. 15). This result is in agreement with the other measurements shown in figure 3.

Figure 4 shows the latitudinal and altitudinal variation of mixing ratio as determined by use of the Bolle-Smith transmission model, the Goody transmission model, and the Elsasser transmission model for cells 1, 3, 5, and 7. (Table VI gives data for all 7 cells.) Each set is consistent and the relative value and change as a function of latitude can be seen. Figure 4 indicates that even though the absolute value of the mixing ratio is in doubt, any of the transmission models will indicate latitudinal trends accurately. For
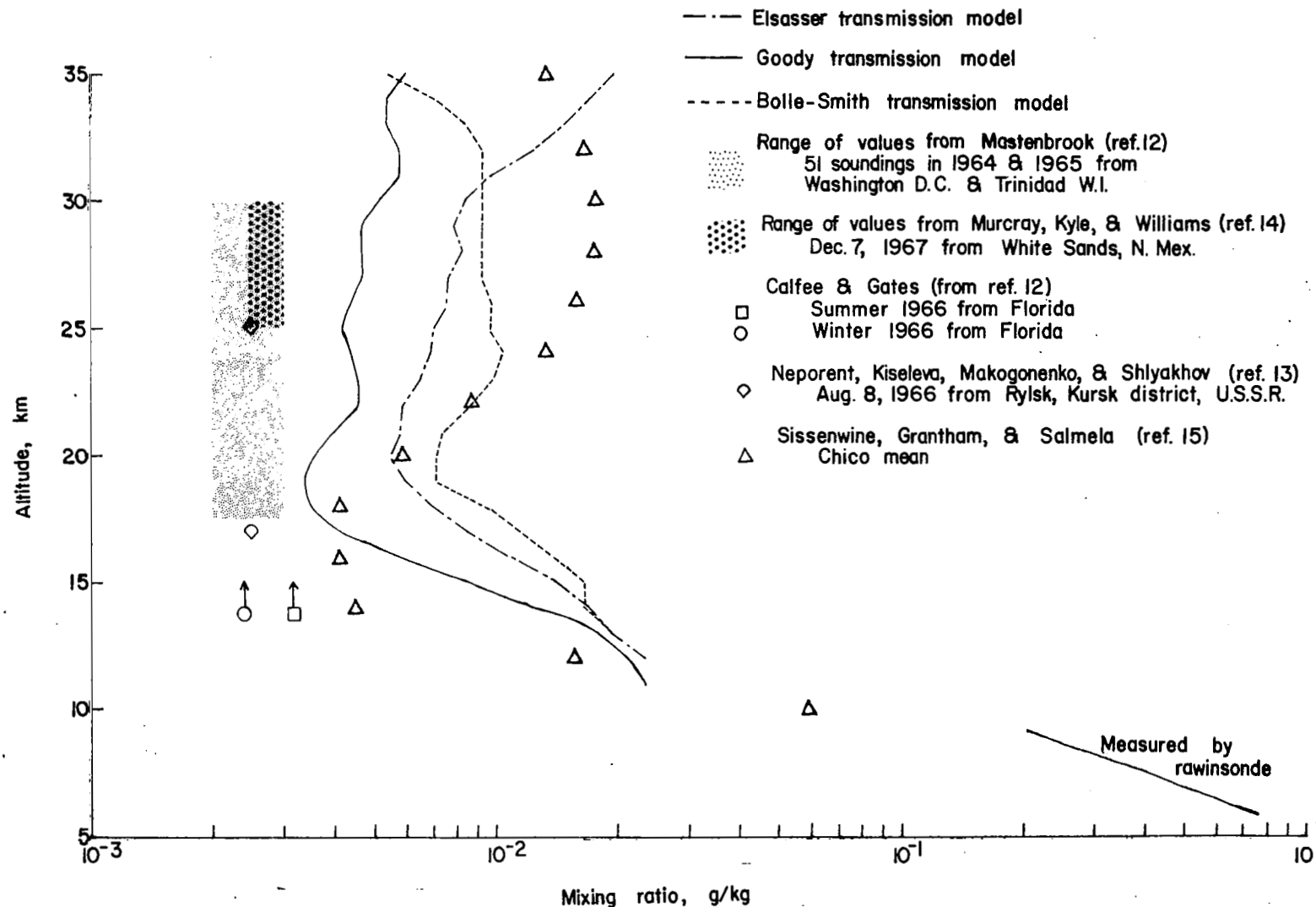
Figure 3.- Inferred and measured mixing ratio for cell 5 from Project Scanner along with other measurements obtained from various references.
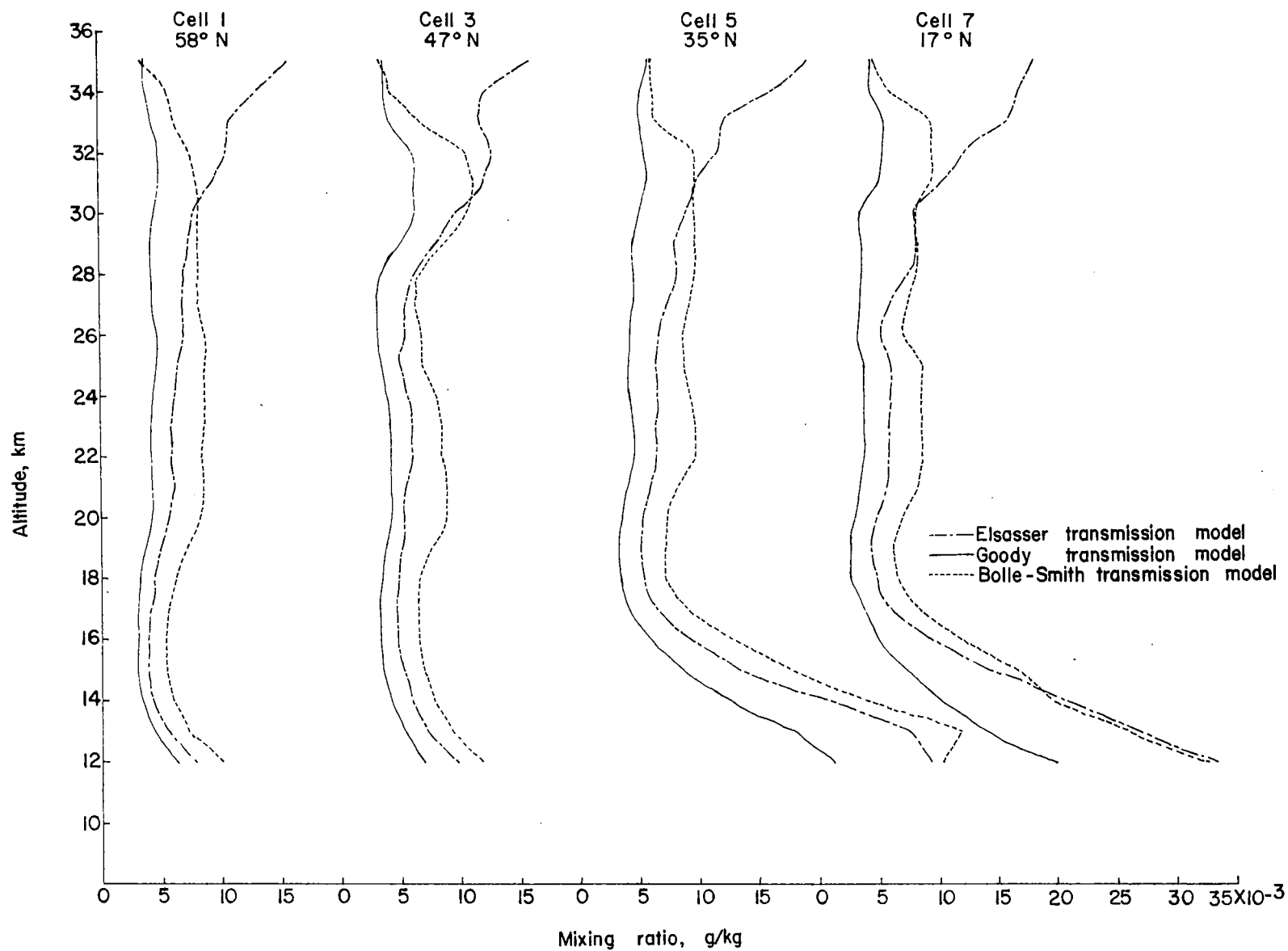
Figure 4.- Comparison of latitudinal variation of inferred mixing ratio
when different transmission models are assumed.

any one transmission model there is no significant variation of mixing ratio above approximately 18 km. Below 18 km, all three transmission models show that a significant variation of mixing ratio does exist and does reflect the large variations that are known to exist in the tropopause. Mixing ratios below 18 km decrease with increasing latitude. As previously indicated, no significance can be attached to the decrease in mixing ratio indicated by the Bolle-Smith transmission model instead of the increase in mixing ratio indicated by the Elsasser mixing ratio in the 30-km region. The 315 cm^{-1} to 475 cm^{-1} bandwidth was not originally chosen for the inference of water-vapor mixing ratio and the transmission model chosen for inference of water-vapor mixing ratio under these given conditions will result in significant changes in the mixing ratio profile above an altitude of approximately 25 km. In another band, such as 200 cm^{-1} to 300 cm^{-1}, the marked change in the mixing ratio profile caused by the choice of the Bolle-Smith transmission model instead of the Elsasser transmission model would occur at a different altitude but it would be present since it is a function of the shape of the chosen transmission curve between $\tau_\nu = 0.9$ and $\tau_\nu = 1.0$. In the two bands examined, it does not appear that the shape of the mixing ratio profile would change significantly as a function of band choice if the Goody transmission model was used.

CONCLUDING REMARKS

The effect of changing the transmission model for the rotational water-vapor band when calculating radiance or when inferring water-vapor mixing has been studied. The radiance was calculated and the mixing ratio was inferred by use of the Elsasser transmission model, the Bolle-Smith transmission model, and the Goody transmission model. The shape of the transmission (τ_ν) curve between 0.9 and 1.0 differed sufficiently between the Elsasser transmission model and the Bolle-Smith transmission model that the shape of the inferred mixing ratio profile is transmission model dependent when τ_ν was in that region. The altitude where $0.9 < \tau_\nu < 1.0$ is frequency dependent; thus, the shape of the inferred mixing ratios as a function of altitude when assuming either the Elsasser transmission model or the Bolle-Smith transmission model is also frequency dependent. There does not appear to be a frequency dependence in the shape of the inferred mixing ratio when the Goody transmission model is used. Coefficients necessary to correct the Goody transmission model for the effect of temperature are also presented.

The effects of inferring water-vapor mixing ratio from NASA's Project Scanner (August 1966) horizon radiance profile data utilizing the Bolle-Smith transmission model and the Goody transmission model are presented and are compared with the mixing ratios from that flight that were inferred by utilizing the Elsasser transmission model. The inferred mixing ratios agree within factors of 2 or 3, the Goody model giving the lowest values. Inferences utilizing each of the transmission models indicate that no significant

latitudinal variations exist above 18 km, and below 18 km they show latitudinal variations that are consistent with the large variations that are known to exist in the tropopause. All the models using the 315 cm^{-1} to 475 cm^{-1} band indicate mixing ratios essentially independent of altitude from above the tropopause to at least 25 km; and the Goody model suggests this constancy may extend to 35 km.

Langley Research Center,
    National Aeronautics and Space Administration,
        Hampton, Va., February 4, 1971.

REFERENCES

1. McKee, Thomas B.; Whitman, Ruth I.; and Davis, Richard E.: Infrared Horizon Profiles for Summer Conditions From Project Scanner. NASA TN D-4741, 1968.

2. Whitman, Ruth I.; McKee, Thomas B.; and Davis, Richard E.: Infrared Horizon Profiles for Winter Conditions From Project Scanner. NASA TN D-4905, 1968.

3. Kondrat'yev, K. Ya.; and Timofeyev, Yu. M.: Numerical Modeling of Transmission Functions for Narrow Spectral Intervals in the $15\mu m$ CO_2 Band. Physics of the Atmosphere and Ocean, Joint Publ. Res. Serv. 48753, Sept. 4, 1969, pp. 52-68.

4. McKee, Thomas B.; Whitman, Ruth I.; and Lambiotte, Jules J., Jr.: A Technique To Infer Atmospheric Water-Vapor Mixing Ratio From Measured Horizon Radiance Profiles. NASA TN D-5252, 1969.

5. House, Frederick B.; and Ohring, George: Inference of Stratospheric Temperature and Moisture Profiles From Observation of the Infrared Horizon. NASA CR-1419, 1969.

6. Elsasser, Walter M.; and Culbertson, Margaret F.: Atmospheric Radiation Tables. Meteorol. Monogr., vol. 4, no. 23, Aug. 1960.

7. Bates, Jerry C.; Hanson, David S.; House, Fred B.; Carpenter, Robert O'B.; and Gille, John C.: The Synthesis of 15μ Infrared Horizon Radiance Profiles From Meteorological Data Inputs. NASA CR-724, 1967.

8. Goody, R.M.: Atmospheric Radiation. I.- Theoretical Basis. Clarendon Press (Oxford), 1964.

9. Rodgers, C. D.; and Walshaw, C. D.: The Computation of Infra-Red Cooling Rate in Planetary Atmospheres. Quart. J. Roy. Meteorol. Soc., vol. 92, no. 391, Jan. 1966, pp. 67-92.

10. Smith, William L.: A Polynomial Representation of Carbon Dioxide and Water Vapor Transmission. ESSA Tech. Rep. NESC47, U.S. Dep. Com., Feb. 1969.

11. Anon.: U.S. Standard Atmosphere, 1962. NASA, U.S. Air Force, and U.S. Weather Bur., Dec. 1962.

12. Mastenbrook. H. J.: Water Vapor Distribution in the Stratosphere and High Troposphere. J. Atmos. Sci., vol. 25, no. 2, Mar. 1968, pp. 299-311.

13. Neporent, B. S.; Kiseleva, M. S.; Makogonenko, A. G.; and Shlyakhov, V. I.: Determination of Moisture in the Atmosphere From Absorption of Solar Radiation. Appl. Opt., vol. 6, no. 11, Nov. 1967, pp. 1845-1850.

14. Murcray, D. G.; Kyle, T. G.; and Williams, W. J.: Distribution of Water Vapor in the Stratosphere as Derived From Setting Sun Absorption Data. J. Geophys. Res., vol. 74, no. 23, Oct. 20, 1969, pp. 5369-5373.

15. Sissenwine, N.; Grantham, D. D.; and Salmela, H. A.: Humidity Up to the Mesopause. AFCRL-68-0550, U.S. Air Force, Oct. 1968. (Available from DDC as AD 679 996.)

TABLE I.- CONSTANTS FOR TEMPERATURE CORRECTION

FOR GOODY TRANSMISSION MODEL

Band, cm^{-1}	$\bar{a}$	$\bar{b}$
0 to 20	-9.1698×10^{-3}	1.6922×10^{-5}
20 to 40	-8.0365	1.1450
40 to 60	-6.2565	1.0581
60 to 80	-4.5274	3.4052×10^{-6}
80 to 100	-4.5991	6.2531
100 to 120	-1.6255	-4.4631
120 to 140	-4.8659×10^{-4}	-6.1700
140 to 160	-9.5400	-1.7472
160 to 180	6.8565×10^{-5}	-2.7554
180 to 200	6.2048×10^{-3}	-2.6306×10^{-5}
200 to 220	-6.7133×10^{-4}	-2.4892×10^{-6}
220 to 240	2.1739×10^{-3}	-1.2110×10^{-5}
240 to 260	3.0253	-1.8678
260 to 280	5.9599	-3.1064
280 to 300	6.6139	-3.1576
300 to 320	8.5968	-4.1172
320 to 340	7.7381	-3.1637
340 to 360	1.2495×10^{-2}	-5.5440
360 to 380	1.5795	-6.0094
380 to 400	1.4916	-7.6087
400 to 420	1.3272	-4.2334
420 to 440	2.1022	-3.6128
440 to 460	1.3408	-2.6505
460 to 480	1.5641	-2.2485
480 to 500	1.2779	-4.4954×10^{-7}
500 to 520	1.7321	1.0652×10^{-3}
520 to 540	1.4252	-3.4652×10^{-5}
540 to 560	1.2783	-3.0347
560 to 580	1.2844	-3.7653
580 to 600	1.7022	-7.4486
600 to 620	1.5927	-4.2620
620 to 640	1.9443	-7.1937
640 to 660	2.2053	-2.5421
660 to 680	1.2236	-2.1281
680 to 700	2.3144	-9.0283
700 to 720	2.0357	-5.2233
720 to 740	1.5172	-4.2996
740 to 760	2.6330	-8.2911
760 to 780	2.2390	-4.9984
780 to 800	1.9945	-5.8346
800 to 820	2.6716	-4.3537
820 to 840	2.0879	-1.8101
840 to 860	2.6050	-6.5905
860 to 880	2.3727	-7.8596
880 to 900	1.7627	-2.0281
900 to 920	3.0795	-1.0238×10^{-4}
920 to 940	2.3201	-4.6785×10^{-5}
940 to 960	2.4398	-6.8687
960 to 980	-2.5104	-1.0168×10^{-4}
980 to 1000	-1.0134×10^{-3}	5.9949×10^{-4}

TABLE II.- U.S. 1962 STANDARD ATMOSPHERE VALUES

$\left[\text{Values from ref. 11; } 1 \text{ mb} = 100 \text{ N/m}^2\right]$

Altitude, km	Temperature, $^{\circ}$K	Pressure, mb
0	288.15	1013.25
2	275.15	795.01
4	262.17	616.60
6	249.19	472.18
8	236.22	356.52
10	223.25	265.00
12	216.65	193.99
14	216.65	141.70
16	216.65	103.53
18	216.65	75.65
20	216.65	55.29
22	218.57	40.47
24	220.56	29.72
26	222.54	21.88
28	224.53	16.16
30	226.51	11.97
32	228.49	8.89
34	233.75	6.63
36	239.28	4.99
38	244.82	3.77
40	250.35	2.87
42	255.88	2.20
44	261.40	1.70

TABLE III.- MIXING RATIO AND CALCULATED RADIANCE PROFILES

Altitude, km	Mixing ratio, g/kg	Tangent height, km	Calculated radiance, 315 cm^{-1} to 475 cm^{-1}, for –			Calculated radiance, 200 cm^{-1} to 300 cm^{-1}, for –		
			Elsasser transmission model, W/m^2-sr	Goody transmission model, W/m^2-sr	Bolle-Smith transmission model, W/m^2-sr	Elsasser transmission model, W/m^2-sr	Goody transmission model, W/m^2-sr	Bolle-Smith transmission model, W/m^2-sr
0	5.0×10^0	0	11.01	11.09	11.18	4.49	4.54	4.53
1	3.0	1	10.96	11.05	11.14	4.48	4.53	4.53
2	1.8	2	10.91	11.00	11.09	4.48	4.53	4.52
3	1.0	3	10.86	10.94	11.03	4.48	4.52	4.52
4	6.0×10^{-1}	4	10.79	10.86	10.96	4.47	4.52	4.51
5	3.5	5	10.68	10.71	10.88	4.47	4.51	4.50
6	2.2	6	10.44	10.42	10.74	4.46	4.50	4.49
7	1.3	7	9.94	9.89	10.35	4.46	4.50	4.48
8	7.6×10^{-2}	8	9.05	9.06	9.38	4.45	4.48	4.47
9	4.5	9	7.83	7.98	7.97	4.44	4.46	4.45
10	2.7	10	6.48	6.82	6.69	4.40	4.40	4.40
11	1.6	11	5.27	5.74	5.29	4.31	4.27	4.23
12	1.0	12	4.33	4.81	4.00	4.14	4.06	3.94
13	9.0×10^{-3}	13	3.77	4.25	3.43	3.98	3.88	3.69
14	8.0	14	3.24	3.71	2.91	3.75	3.64	3.41
15	7.1	15	2.77	3.21	2.45	3.48	3.37	3.12
16	6.3	16	2.35	2.76	2.06	3.19	3.09	2.83
17	5.6	17	2.00	2.37	1.74	2.89	2.80	2.55
18	5.0	18	1.70	2.05	1.48	2.60	2.52	2.28
19	5.0	19	1.48	1.81	1.30	2.37	2.29	2.06
20	5.0	20	1.29	1.60	1.14	2.14	2.08	1.86
21	5.0	21	1.13	1.41	1.01	1.93	1.88	1.66
22	5.0	22	.98	1.25	.90	1.74	1.69	1.48
23	5.0	23	.85	1.10	.80	1.55	1.52	1.31
24	5.0	24	.73	.98	.71	1.38	1.37	1.16
25	5.0	25	.62	.87	.64	1.23	1.23	1.03
26	5.0	26	.53	.77	.58	1.10	1.10	.91
27	5.0	27	.46	.69	.52	.98	.99	.81
28	5.0	28	.39	.62	.49	.88	.90	.72
29	5.0	29	.34	.57	.44	.80	.83	.66
30	5.0	30	.29	.53	.41	.74	.76	.60
31	6.3	31	.27	.50	.40	.70	.73	.57
32	7.8	32	.25	.48	.38	.66	.70	.54
33	9.8	33	.22	.45	.37	.63	.66	.51
34	1.2×10^{-2}	34	.19	.42	.35	.58	.62	.47
35	1.5	35	.17	.39	.33	.54	.57	.43
36	1.5					.47	.51	.38
37	1.5					.41	.45	.34
38	1.5					.35	.40	.30
39	1.5					.29	.36	.26
40	1.5					.24	.32	.23
41	1.5					.20	.28	.21
42	1.5					.15	.25	.18
43	1.5					.11	.22	.16
44	1.5					.08	.20	.15
45	1.5					.05	.18	.13

TABLE IV.- MEASURED RADIANCE PROFILES FROM THE

PROJECT SCANNER FLIGHT IN AUGUST 1966

[Data from ref. 1; 315 cm^{-1} to 475 cm^{-1} spectral interval]

Tangent height, km	Radiance profiles, W/m^2-sr, for cell —						
	1	2	3	4	5	6	7
10	6.57	6.27	6.02	6.11	7.01	7.18	7.74
11	5.52	5.38	5.23	5.51	6.32	6.26	6.79
12	4.47	4.53	4.45	4.88	5.54	5.31	5.75
13	3.66	3.82	3.76	4.25	4.72	4.41	4.71
14	3.12	3.28	3.21	3.64	3.93	3.64	3.74
15	2.76	2.86	2.78	3.09	3.22	3.00	2.92
16	2.48	2.52	2.44	2.63	2.65	2.49	2.31
17	2.24	2.25	2.18	2.29	2.22	2.11	1.89
18	2.02	2.03	1.96	2.04	1.92	1.83	1.64
19	1.84	1.84	1.76	1.84	1.71	1.61	1.48
20	1.67	1.64	1.58	1.68	1.54	1.43	1.36
21	1.48	1.46	1.42	1.52	1.40	1.29	1.25
22	1.29	1.29	1.26	1.37	1.27	1.16	1.12
23	1.14	1.15	1.10	1.22	1.12	1.05	.99
24	1.02	1.02	.95	1.09	.99	.95	.88
25	.91	.90	.82	.99	.87	.85	.79
26	.81	.80	.74	.90	.78	.76	.68
27	.70	.70	.67	.82	.70	.66	.61
28	.61	.61	.61	.74	.63	.58	.56
29	.54	.52	.58	.67	.56	.51	.50
30	.48	.45	.53	.60	.51	.46	.44
31	.43	.40	.47	.54	.46	.42	.42
32	.38	.36	.40	.47	.42	.39	.38
33	.32	.31	.32	.40	.36	.35	.34
34	.28	.27	.27	.35	.32	.31	.29
35	.24	.23	.24	.32	.29	.26	.24

TABLE V.- MODEL ATMOSPHERES DERIVED FROM METEOROLOGICAL DATA

$$\left[\text{From ref. 1; 1 mb} = 100 \text{ N/m}^2\right]$$

Altitude, km	Cell 1 (58° N 68° W)		Cell 2 (53° N 60° W)		Cell 3 (47° N 57° W)		Cell 4 (43° N 45° W)	
	Temperature, °K	Pressure, mb	Temperature, °K	Pressure, mb	Temperature, °K	Pressure, mb	Temperature, °K	Pressure, mb
0	288.0	1010.000	288.0	1010.000	286.0	1012.000	294.0	1025.000
2	277.0	800.511	277.4	800.575	280.1	807.089	284.3	811.321
4	263.2	626.923	264.2	625.462	268.4	634.169	278.2	637.879
6	250.9	477.778	251.3	477.778	257.3	485.542	260.8	489.881
8	234.7	362.245	237.1	364.762	243.3	371.429	246.5	375.253
10	221.7	267.500	221.7	268.487	230.0	277.642	231.3	281.707
12	224.9	196.296	223.8	196.543	217.1	203.652	213.9	207.343
14	224.0	145.370	221.2	145.000	218.0	149.000	213.1	148.810
16	224.0	111.025	222.7	106.884	218.0	110.075	216.5	105.932
18	224.3	79.783	224.0	79.690	219.6	80.161	219.5	81.053
20	225.0	59.065	225.0	59.039	223.1	56.319	222.0	59.115
22	225.6	43.153	225.9	42.702	224.6	43.495	222.6	43.420
24	227.6	31.922	226.0	31.787	225.8	32.132	223.0	31.998
26	232.0	23.590	227.0	23.475	227.2	23.761	225.2	23.583
28	233.6	17.715	228.3	17.491	230.6	17.690	228.1	17.676
30	235.0	13.200	235.0	12.950	237.0	13.170	232.7	13.151
32	237.8	9.910	237.0	9.720	237.0	9.900	238.0	9.740
34	240.6	7.470	240.0	7.320	240.0	7.450	241.0	7.340
36	245.6	5.650	244.0	5.530	245.0	5.640	246.0	5.560
38	252.8	4.310	251.0	4.210	251.0	4.290	250.0	4.240
40	260.0	3.310	258.0	3.230	257.0	3.290	256.0	3.240
42	262.8	2.556	261.0	2.490	260.0	2.535	260.0	2.498
44	256.6	1.971	264.0	1.920	263.0	1.959	263.0	1.930
46	267.0	1.523	265.0	1.491	265.0	1.517	265.0	1.495
48	266.0	1.183	264.0	1.156	265.0	1.177	264.0	1.159
50	265.0	.918	263.0	.895	262.0	.911	262.0	.897
52	261.4	.710	259.0	.691	260.0	.704	261.0	.694
54	258.8	.548	256.0	.532	257.0	.543	260.0	.536
56	257.5	.442	254.7	.431	255.0	.439	257.0	.433
58	256.3	.336	253.3	.331	253.0	.334	254.0	.331
60	255.0	.230	252.0	.230	251.0	.230	251.0	.228
62	246.2	.180	244.4	.180	243.8	.179	243.0	.178
64	237.4	.130	236.8	.130	236.6	.128	235.0	.128
66	229.0	.095	229.0	.095	229.0	.093	227.6	.093
68	221.0	.074	221.0	.074	221.0	.073	220.8	.073
70	213.0	.053	213.0	.053	213.0	.053	214.0	.053

TABLE V.- MODEL ATOMSPHERES DERIVED FROM METEOROLOGICAL DATA – Concluded

$\left[\text{From ref. 1; } 1 \text{ mb} = 100 \text{ N}/\text{m}^2\right]$

Altitude, km	Cell 5 (35° N 48° W)		Cell 6 (21° N 55° W)		Cell 7 (17° N 60° W)	
	Temperature, °K	Pressure, mb	Temperature, °K	Pressure, mb	Temperature, °K	Pressure, mb
0	299.0	1023.000	301.0	1016.000	301.0	1016.000
2	284.1	785.377	287.8	808.129	287.8	808.129
4	274.8	639.370	275.2	637.736	275.2	637.736
6	264.5	495.294	259.7	492.669	259.7	492.669
8	250.5	380.612	252.7	379.412	252.7	379.412
10	235.3	287.600	237.1	286.800	237.1	286.800
12	218.2	213.194	220.9	213.014	220.9	213.014
14	204.0	155.000	209.0	154.749	209.0	154.749
16	207.5	112.398	201.0	110.853	201.0	110.853
18	213.0	81.087	205.0	78.659	205.0	78.659
20	217.1	59.074	212.6	57.080	212.6	57.080
22	220.5	43.253	217.5	41.525	217.5	41.525
24	222.7	31.744	219.0	30.412	219.0	30.422
26	225.6	23.250	227.0	22.585	227.0	22.585
28	227.7	17.360	227.7	16.833	227.7	16.839
30	230.0	12.830	227.0	12.390	225.0	12.380
32	239.0	9.620	235.0	9.250	233.0	9.220
34	244.0	7.270	242.0	6.970	241.0	6.930
36	248.0	5.520	247.0	5.290	247.0	5.260
38	251.0	4.220	250.0	4.030	250.0	4.010
40	254.0	3.230	253.0	3.080	253.0	3.070
42	259.0	2.481	259.0	2.370	259.0	2.358
44	264.0	1.917	266.0	1.834	260.0	1.825
46	265.0	1.487	268.0	1.426	270.0	1.420
48	264.0	1.153	265.0	1.108	269.0	1.107
50	262.0	.893	262.0	.859	262.0	.859
52	265.0	.692	267.0	.666	268.0	.667
54	268.0	.538	273.0	.520	273.0	.520
56	264.0	.434	267.0	.422	266.3	.425
58	260.0	.329	261.0	.323	259.7	.330
60	256.0	.225	255.0	.225	253.0	.235
62	248.4	.181	247.8	.181	246.2	.189
64	240.8	.136	240.6	.136	239.4	.143
66	233.4	.102	233.2	.102	232.6	.108
68	226.2	.077	225.6	.077	225.8	.083
70	219.0	.053	218.0	.053	219.0	.058

TABLE VI.- INFERRED MIXING RATIOS USING THREE TRANSMISSION MODELS

Altitude, km	Mixing ratios, g/kg, for cell —											
	1			2			3			4		
	Transmission model			Transmission model			Transmission model			Transmission model		
	Elsasser	Goody	Bolle-Smith	Elsasser	Goody	Bolle-Smith	Elsasser	Goody	Bolle-Smith	Elsasser	Goody	Bolle-Smith
12	7.9×10^{-3}	6.3×10^{-3}	10.0×10^{-3}	8.6×10^{-3}	6.9×10^{-3}	11.0×10^{-3}	9.7×10^{-3}	6.9×10^{-3}	1.16×10^{-3}	15.6×10^{-3}	9.4×10^{-3}	14.8×10^{-4}
13	5.4	4.3	7.1	6.8	5.2	8.7	7.2	5.3	9.2	13.3	8.5	14.8
14	4.3	3.4	5.8	5.7	4.3	7.5	5.9	4.3	7.7	11.4	8.0	14.6
15	3.9	3.0	5.4	5.0	3.6	6.7	5.1	3.5	6.8	9.2	7.6	14.4
16	3.9	3.0	5.3	4.6	3.4	6.3	4.7	3.3	6.5	6.5	5.2	10.0
17	4.1	3.1	5.6	4.5	3.4	6.2	4.7	3.3	6.5	5.3	3.7	7.1
18	4.4	3.3	6.1	4.8	3.6	6.6	4.9	3.5	6.6	5.0	3.5	7.0
19	4.9	3.7	7.1	5.2	3.9	7.5	5.2	3.8	7.5	5.1	3.6	7.2
20	5.7	4.2	8.3	5.5	4.1	7.7	5.3	4.3	8.9	5.7	4.2	8.1
21	6.2	4.3	8.6	6.0	4.3	8.5	5.6	4.3	8.9	6.5	4.6	9.0
22	5.8	4.1	8.4	6.0	4.3	8.8	6.1	4.3	8.5	6.9	4.9	10.0
23	5.8	4.1	8.7	6.4	4.5	9.3	6.1	4.2	8.5	7.0	4.9	10.3
24	6.2	4.4	8.7	6.7	4.7	9.7	5.7	3.8	8.0	7.1	4.9	10.3
25	6.5	4.6	8.7	7.1	4.9	10.1	5.2	3.3	6.9	7.8	5.2	11.1
26	7.0	4.6	8.7	7.9	5.1	10.5	5.5	3.3	6.9	8.7	5.7	12.2
27	6.8	4.3	8.2	8.4	5.1	10.5	5.7	3.3	6.4	9.6	6.3	13.2
28	7.0	4.3	8.2	8.6	4.8	9.9	6.0	3.6	6.4	9.7	6.7	14.0
29	7.5	4.3	8.2	7.9	4.1	7.6	8.1	5.1	8.5	10.9	7.2	14.8
30	7.8	4.6	8.2	7.2	4.1	7.0	9.8	6.4	10.7	12.1	7.8	14.8
31	9.4	5.0	8.2	8.4	4.7	7.0	12.2	6.4	11.3	14.2	8.2	14.8
32	10.7	5.0	7.6	10.2	4.7	7.0	12.9	6.4	10.6	14.7	7.5	13.4
33	10.8	4.3	6.3	11.1	4.3	6.1	11.2	4.4	6.9	14.4	6.4	9.7
34	13.2	3.9	5.6	13.6	3.8	5.4	12.3	3.9	4.3	17.0	6.4	8.8
35	15.8	3.9	3.5	16.1	3.8	3.2	16.1	3.9	3.5	22.3	7.3	8.8
Latitude, °N	58			53			47			43		
Longitude, °W	68			60			57			45		
Tropopause altitude, km	10			10			12			14		

TABLE VI.- INFERRED MIXING RATIOS USING THREE TRANSMISSION MODELS – Concluded

Altitude, km	Mixing ratios, g/kg, for cell								
	5			6			7		
	Transmission model			Transmission model			Transmission model		
	Elsasser	Goody	Bolle-Smith	Elsasser	Goody	Bolle-Smith	Elsasser	Goody	Bolle-Smith
12	29.3×10^{-3}	21.1×10^{-3}	30.4×10^{-3}	22.9×10^{-3}	15.3×10^{-3}	23.1×10^{-3}	33.4×10^{-3}	19.8×10^{-3}	32.6×10^{-3}
13	27.6	17.9	31.9	19.5	11.4	19.2	26.8	14.2	25.8
14	20.9	12.5	24.1	17.0	9.2	16.3	20.4	10.2	19.5
15	13.4	8.5	17.6	14.0	7.8	16.3	14.1	7.3	16.5
16	9.3	5.8	12.6	10.7	6.0	13.6	9.2	4.8	11.8
17	6.6	4.2	8.8	8.5	4.8	11.2	6.0	3.3	8.2
18	5.4	3.5	7.3	7.0	4.0	9.5	4.8	2.6	6.5
19	5.1	3.4	7.3	6.0	3.6	8.1	4.4	2.6	6.2
20	5.3	3.6	7.3	5.5	3.5	8.1	4.8	3.0	7.0
21	6.0	4.0	8.2	5.8	3.7	8.4	5.7	3.5	8.4
22	6.5	4.6	9.8	5.9	3.9	8.6	5.9	3.8	8.7
23	6.5	4.6	9.8	6.5	4.3	9.9	6.0	3.8	8.7
24	6.6	4.4	9.4	6.9	4.6	10.3	6.1	3.8	8.7
25	6.5	4.2	8.8	7.0	4.9	9.7	6.2	3.8	8.7
26	6.9	4.4	8.8	7.5	4.9	9.7	5.4	3.4	7.2
27	7.6	4.7	9.3	7.6	4.6	9.2	6.1	3.6	7.6
28	8.3	4.7	9.9	8.2	4.3	9.2	7.7	3.9	8.3
29	8.1	4.7	9.9	7.9	4.3	9.2	7.9	3.9	8.3
30	9.1	5.2	9.9	8.4	4.3	9.2	7.6	3.9	8.3
31	10.0	5.8	9.9	9.6	4.9	9.2	10.5	5.3	9.6
32	11.9	5.8	9.9	12.2	5.9	9.2	12.5	5.7	9.6
33	12.2	5.4	7.1	14.6	5.9	8.4	16.2	5.7	9.6
34	16.3	5.4	6.4	17.0	5.9	7.0	17.0	4.6	6.2
35	19.4	6.0	6.4	19.3	5.4	5.4	18.3	4.6	4.8

Latitude, °N 35   21   17

Longitude, °W 48   55   60

Tropopause altitude, km 14   16   16